CME LIVE OPEN ACCESS

Journal of Cancer Research

Research Article

ISSN: 2578-3726

Targeting Glycolysis and p53-Dependent Fate Control in Lung Squamous Cell Carcinoma Synergistic Disruption of the GLUT1/LDH-A Axis and Restoration of MT1/TP53 Signaling by Brassinin Kevetrin Hydrochloride and Melatonin

Alexandre Tavartkiladze[1,2,4*], Russel J. Reiter[3], Ruite Lou[4], Dinara Kasradze[2], Nana Okrostsvaridze[3], Pati Revazishvili[2], Maia Maisuradze[2], Irine Andronikashvili[2], Pirdara Nozadze[2], Levan Tavartkiladze[2], Rusudan Khutsishvili[2], David Jinchveladze[2] and Givi Tavartkiladze[2]

[1]*Department of Medical Oncology, Tbilisi State Medical University, Tbilisi, Georgia.*

[2]*Department of Personalized Medicine, Tbilisi State Medical University, Tbilisi, Georgia.*

[3]*Department of Cellular & Structural Biology, University of Texas Health Science Center, San Antonio, USA.*

[4]*Department of Biotechnology, Foconsci Chemical Industry, Shandong, China.*

Corresponding Author: Alexandre Tavartkiladze, Department of Medical Oncology, Tbilisi State Medical University, Tbilisi, Georgia.

Received: 2025 Nov 05 **Accepted:** 2025 Dec 24 **Published:** 2025 Dec 04

Simple Summary

Lung squamous cell carcinoma (LUSC) is highly dependent on glycolysis and often expresses high levels of GLUT1 and LDH-A while harboring TP53 mutations [1–6]. Melatonin receptor signaling (MT1/MT2) can also be epigenetically silenced in squamous tumors [10–12]. In this preclinical work we combined three agents—**brassinin, Kevetrin hydrochloride,** and melatonin—to simultaneously inhibit STAT3/PI3K/mTOR signaling, re-activate p53, normalize MT1 signaling, and shut down the GLUT1/LDH-A axis. In LUSC cells carrying an **MTNR1A promoter polymorphism rs2119882 (–184T/C)** and mutant TP53, 14 days of triple treatment reduced glycolysis, restored mitochondrial membrane potential, re-engaged p53 dependent apoptosis and, importantly, **normalized and overexpressed MT1** to levels comparable to matched normal bronchial squamous epithelium (Figures 2–5).

Abstract

Background: *LUSC shows a strongly glycolytic phenotype with high GLUT1 and LDH-A expression and frequent TP53 mutations [1–6]. Our previous clinical study in triple-negative breast cancer (TNBC) demonstrated that dual targeting of GLUT1 and LDH-A with phloretin and melatonin can reprogram tumor metabolism and induce regression [16]. Here we investigate a more comprehensive three-agent regimen—**brassinin, Kevetrin HCl,** and **melatonin**—in LUSC cultures harboring an **MTNR1A rs2119882 (–184T/C)** promoter polymorphism and mutant TP53, aiming to simultaneously block glycolysis, restore p53 function and normalize MT1 signaling.*

Methods: *Primary LUSC cultures with rs2119882 (–184T/C) and mutant TP53, and matched normal bronchial squamous epithelium (reference MTNR1A promoter, wild-type TP53) were established. Cells were exposed for 14 days to melatonin + Kevetrin HCl + brassinin (triple), single agents and doublets. Viability, clonogenicity and synergy (Chou–Talalay combination index, CI) were assessed (Table 4, Figure 6) [25]. GLUT1 and LDH-A mRNA/protein were quantified (Figure 3), together with glucose uptake and lactate release. Mitochondrial membrane potential (ΔΨm) was measured by JC-10/JC-1 assays (Figure 2). MTNR1A (MT1) mRNA and protein were evaluated by RT-qPCR and immunofluorescence (IF) (Figure 4). Histone marks (H3K9me3, H3K27ac, H3K4me3) at the MTNR1A promoter were analyzed by ChIP-qPCR. p53 pathway activity was studied by qPCR and Western blotting of p21, PUMA and other targets (Figure 5); TP53 resequencing assessed whether sequence reversion occurred.*

Results: *The triple regimen produced strong synergy (CI 0.3–0.7 across ED_{25}–ED_{90}) and reduced viability and clonogenicity more than any single agent or doublet (Figure 6, Table 4). GLUT1 and LDH-A expression decreased significantly at both mRNA*

and protein levels, with concomitant reductions in glucose uptake and lactate release (Figure 3). ΔΨm, which was low at baseline, became restored in triple-treated cells, as indicated by a 2–3-fold increase in JC-10 red/green ratio (Figure 2). p21 and PUMA were robustly up-regulated, cleaved caspase-3 increased, and Annexin V positivity rose, indicating restored p53-dependent apoptosis (Figure 5). In rs2119882-positive LUSC cells, MT1 was weakly detectable at baseline but became strongly expressed after triple treatment, reaching intensities comparable to those in normal epithelium (Figure 4). ChIP-qPCR at the MTNR1A promoter showed a switch from a repressive to an active histone mark profile (H3K9me3↓, H3K4me3/H3K27ac↑). No TP53 sequence reversion was observed, consistent with functional p53 restoration rather than genetic correction.

Conclusions: *Combined targeting of* ***STAT3/PI3K/mTOR, p53, MT1 signaling*** *and the* ***GLUT1/LDH-A axis*** *with brassinin, Kevetrin HCl and melatonin produces strong synergistic anti-tumor effects in LUSC, including suppression of glycolysis, mitochondrial repolarization, p53 pathway reactivation and epigenetic normalization of MTNR1A/MT1. In rs2119882-positive cultures this amounts to a partial reverse transformation toward an apoptosis-competent, quasi-normal phenotype. These results justify further in vivo and translational investigation of this triple regimen, with* ***MTNR1A promoter status*** *and* ***p53 functional*** *readouts as candidate biomarkers.*

Keywords: Lung Squamous Cell Carcinoma, Glycolysis, GLUT1, LDH-A, p53, MTNR1A, MT1, Brassinin, Kevetrin, Melatonin, Mitochondrial Membrane Potential, Warburg Effect, Chou Talalay Synergy

1. Introduction

Cancer cells typically favor aerobic glycolysis ("Warburg effect") over oxidative phosphorylation even in the presence of oxygen [1,2]. This metabolic shift supports rapid ATP generation and diversion of glycolytic intermediates into biosynthetic pathways but produces excessive lactate and acidifies the tumor microenvironment, promoting invasion, angiogenesis and immune evasion [1,2]. In **non-small cell lung cancer (NSCLC)**—and particularly in the squamous subtype (LUSC)—this phenotype is pronounced [3]. The facilitative transporter **GLUT1 (SLC2A1)** is a major gatekeeper of glucose influx in NSCLC, with high GLUT1 expression correlating with increased ^18F-FDG uptake and adverse prognosis [3,4]. Downstream, lactate dehydrogenase A (LDH-A) converts pyruvate to lactate, regenerates NAD^+, and enables sustained glycolytic flux; LDH-A overexpression has been associated with tumor hypoxia and poor outcome in NSCLC [5]. Thus, the **GLUT1/LDH-A axis** represents a central vulnerability in glycolysis-addicted tumors. In parallel, the tumor suppressor **TP53** is mutated in roughly 80% of LUSC [6]. Wild-type p53 negatively regulates glycolysis by down-regulating GLUT1/GLUT4, inducing **TIGAR** (which lowers fructose-2,6-bisphosphate and inhibits PFK-1), up-regulating **SCO2** (required for mitochondrial complex IV assembly), and suppressing LDH-A expression [7-9]. p53 therefore promotes OXPHOS and constrains the Warburg program. When p53 function is lost, glycolytic overdrive and mitochondrial dysfunction are favored.

1.1. Melatonin Receptors and Mtnr1a Silencing in Squamous Cancers

Melatonin is an indoleamine produced mainly by the pineal gland; it functions as a hormone, autacoid and paracoid with strong antioxidant and anti-inflammatory properties. Beyond its chronobiotic actions, melatonin exerts oncostatic effects by modulating mitochondrial function, redox balance and cell cycle. These effects are transduced in part by its G protein coupled receptors **MT1 (MTNR1A)** and **MT2 (MTNR1B)**. Multiple squamous carcinomas, including **oral squamous-cell carcinoma**, show epigenetic silencing of **MTNR1A**, often via promoter hypermethylation and repressive histone marks [10,11]. In NSCLC, MT1 and MT2 expression has been associated with tumor differentiation and patient outcome, suggesting a functional receptor axis in lung cancer as well [12]. Loss of MT1/MT2 may thus deprive cells of melatonin's anti-proliferative and anti-Warburg signaling [13–15].

1.2. Building on Clinical Work in TNBC

In a recent clinical-translational study in **triple-negative breast cancer (TNBC)**, our group combined a GLUT1 inhibitor (**phloretin**) with high-dose **melatonin** and observed systemic metabolic reprogramming and meaningful tumor regression [16]. We documented reductions in glycolytic markers, increases in OXPHOS indicators and clinical responses in a majority of treated patients [16]. That work established a proof-of-concept that simultaneous GLUT1 and LDH-A targeting is clinically feasible. Given LUSC's strong glycolytic dependence and high TP53 mutation burden, we hypothesized that a **deeper, three-axis intervention** might yield even stronger metabolic and phenotypic reprogramming than in TNBC.

1.3. Rationale for Brassinin + Kevetrin HCl + Melatonin

Our triple regimen consists of

- **Brassinin** – a cruciferous phytoalexin with anticancer activity. In lung cancer models, brassinin inhibits **STAT3** signaling by up-regulating negative regulators **PIAS3** and **SOCS3**, suppresses **PI3K/AKT/mTOR/S6K1**, and sensitizes xenografts to paclitaxel [17-19]. Through these actions it indirectly down-modulates glycolytic drivers and survival pathways.
- **Kevetrin HCl** – an investigational small molecule that **activates or stabilizes wild-type p53** and can down-modulate mutant p53 in certain contexts [20-22]. Kevetrin induces p21 and PUMA, causes cell-cycle arrest and apoptosis, and modulates MDM2–p53 dynamics [20-22]. By re-engaging p53, Kevetrin should restore negative regulation of GLUT1/LDH-A and promote OXPHOS [7-9].
- **Melatonin** – a receptor-dependent and independent

oncostatic agent that suppresses **HIF-1α,** decreases **GLUT1** and **LDH-A,** and enhances mitochondrial respiration through SIRT3–PDH pathway [13-15,23,24]. Melatonin acts via MT1/MT2 and as a direct scavenger of reactive oxygen and nitrogen species [13,23,24].

We reasoned that these agents together could simultaneously:

- Block **IL-6/STAT3** and **PI3K/AKT/mTOR** (brassinin) (Figure 1),
- Restore **p53** transcriptional programs (Kevetrin) (Figures 1 and 5),
- Stabilize and amplify **melatonin receptor signaling** (melatonin, with MT1 re-expression) (Figures 1 and 4),
- Suppress **GLUT1/LDH-A** at multiple regulatory levels (Figures 1–3).

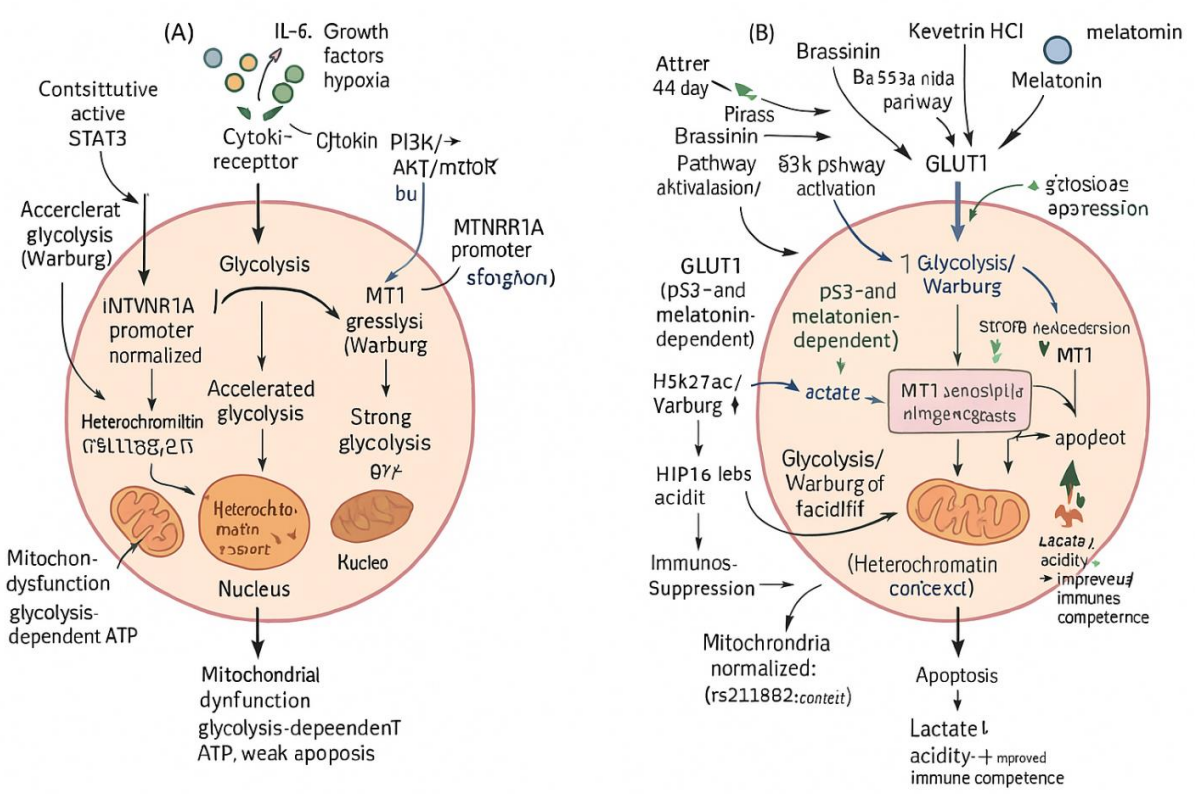

Figure 1: Triple-Agent Mechanism Targeting STAT3/PI3K–p53–MT1 Axes in LUSC

(A) Baseline lung squamous cell carcinoma (LUSC) shows constitutive IL-6/STAT3 and PI3K/AKT/mTOR activation, high GLUT1-mediated glucose influx, and LDH-A–driven lactate production (Warburg effect). The MTNR1A promoter carries the rs2119882 (−184T/C) variant in a repressed, heterochromatic state, with weak MT1 expression; TP53 is mutant and apoptosis-resistant. Mitochondria are depolarized and glycolysis-dependent.

(B) After 14-day combined exposure to brassinin, Kevetrin hydrochloride and melatonin, STAT3 and PI3K/AKT/mTOR activity are reduced, GLUT1 and LDH-A expression decline, and glycolytic flux and lactate release fall. Kevetrin restores p53 functional activity (p21, PUMA, TIGAR, SCO2, RRAD), driving a shift from glycolysis toward oxidative phosphorylation (OXPHOS). Concurrently, the MTNR1A promoter undergoes euchromatinization with MT1 overexpression, enabling strong melatonin–MT1 signaling that further suppresses HIF-1α/GLUT1/LDH-A and stabilizes mitochondria. Together, these changes repolarize mitochondria, promote cytochrome-c release and caspase-dependent apoptosis, reduce tumor-derived lactate, and move LUSC cells toward an apoptosis-competent, quasi-normal phenotype.

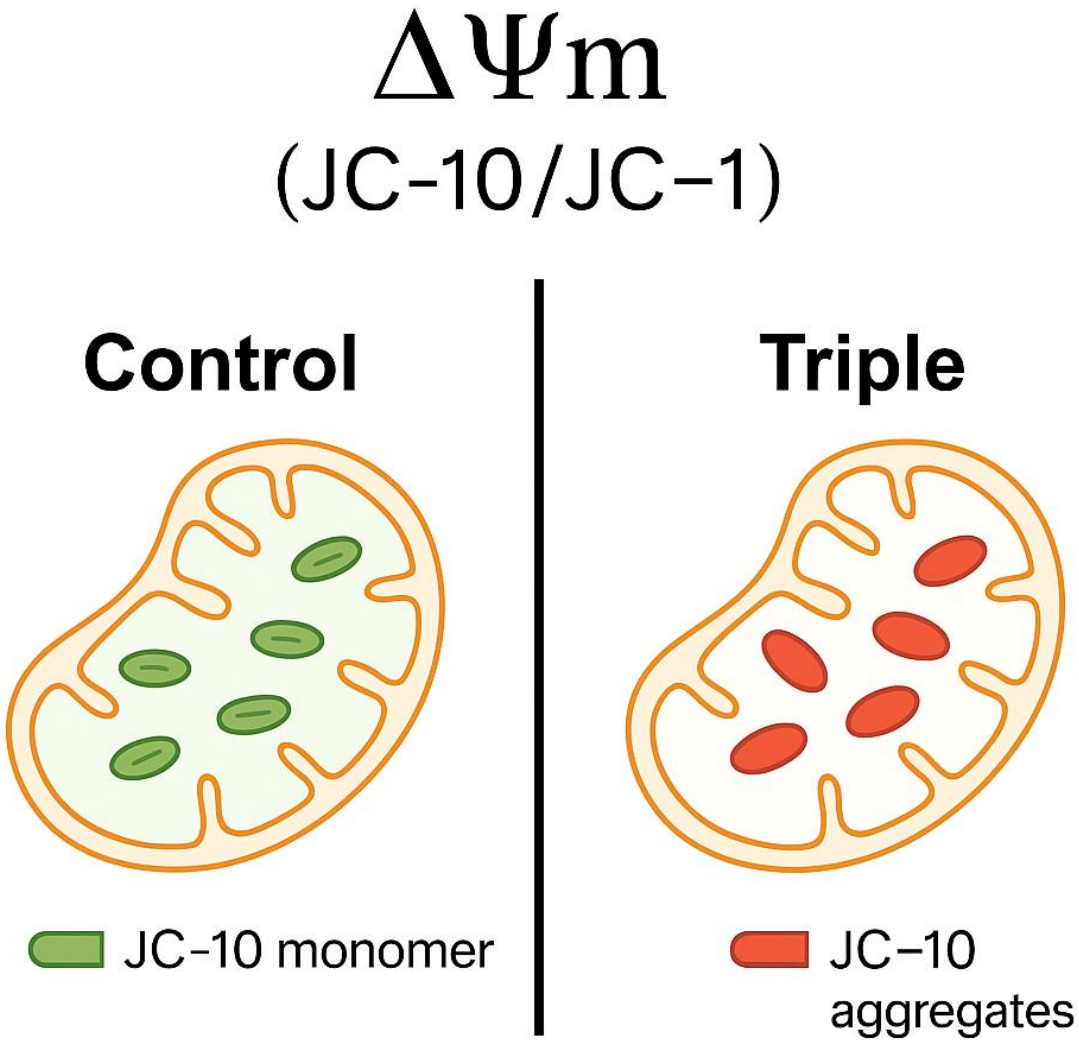

Figure 2: Mitochondrial Membrane Potential (ΔΨm) Measured by JC-10/JC-1 in Control Vs Triple-Treated LUSC Cells. Schematic or Representative Images Illustrating Mitochondria in Control Cells (predominantly Green JC-10 or JC-1 Monomer Signal, Depolarized ΔΨm) and in Triple-Treated Cells (Predominantly Red Aggregate Signal, Repolarized ΔΨm). Bar Graph Inset Shows Quantitative Red/Green Fluorescence Ratios (Mean ± SEM, n ≥ 3)

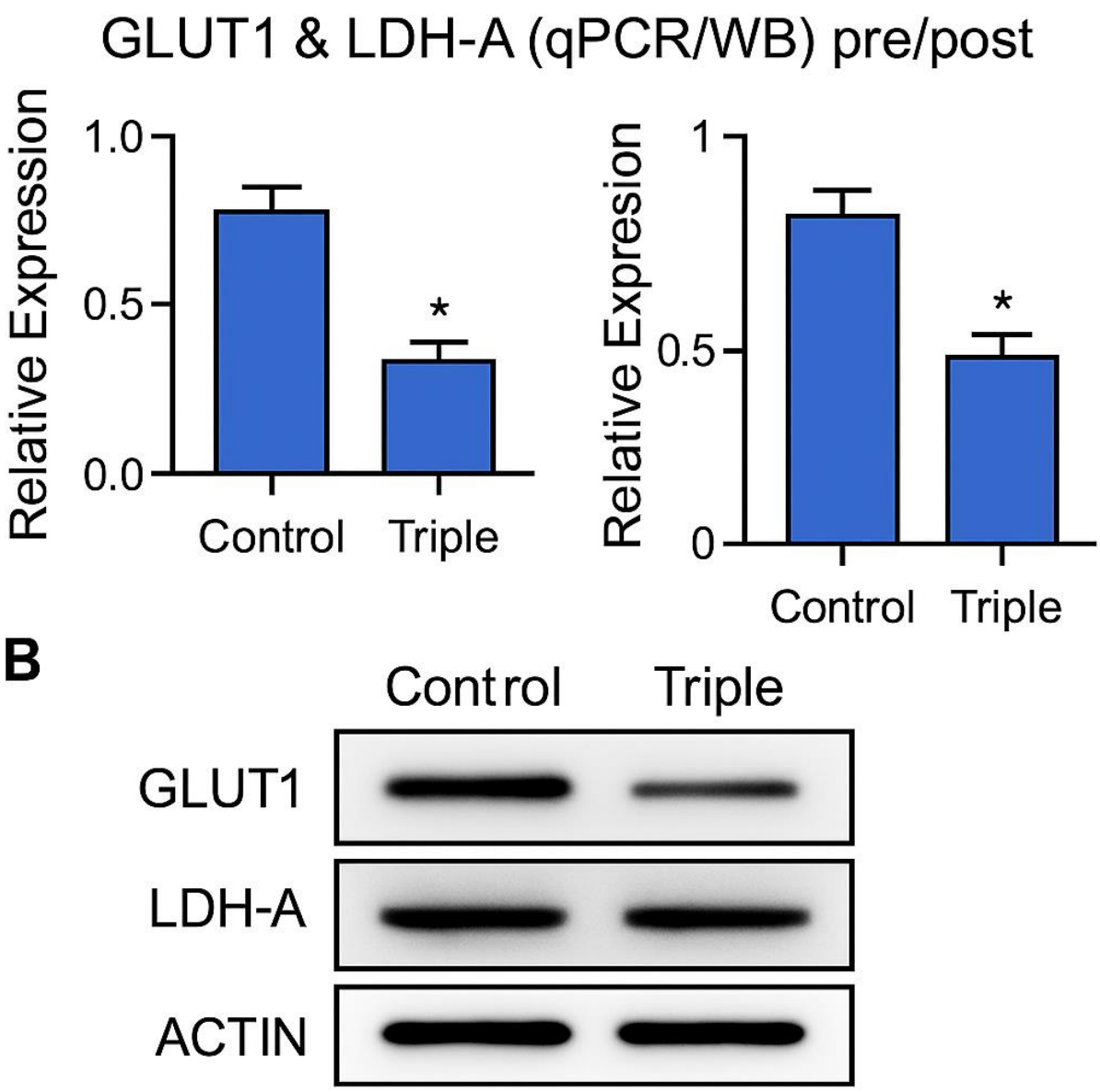

Figure 3: GLUT1 and LDH-A Expression Before and After Triple Treatment. (A) qPCR Data Showing Relative GLUT1 and LDH-A mRNA Expression in Control vs Triple-Treated LUSC Cells. (B) Representative Western Blots and Densitometric Quantification of GLUT1 and LDH-A Protein Levels Normalized to β-Actin. Asterisks Indicate Significant Differences (p < 0.01)**

1.4. Focus on MTNR1A Promoter Polymorphism rs2119882 (−184T/C)

In our LUSC cultures we identified the **MTNR1A promoter polymorphism rs2119882 (−184T/C)**. At baseline, these tumor cells exhibited weak MT1 expression, while matched normal bronchial squamous epithelium (reference MTNR1A promoter) had robust MT1 expression (Figure 4). Given previous data that MTNR1A can be epigenetically silenced in squamous cancers [10,11], we hypothesized that rs2119882 might function as a **therapeutically sensitive gatekeeper**: under malignant conditions it aligns with repression, but under the triple regimen it may become permissive.

The goals of this study were therefore to determine whether the brassinin + Kevetrin HCl + melatonin combination can:

- Synergistically reduce LUSC viability and clonogenicity (Figure 6, Table 4);
- Suppress GLUT1/LDH-A expression and glycolytic flux (Figure 3);
- Restore mitochondrial membrane potential and apoptosis (Figures 2 and 5);
- Normalize MTNR1A promoter activity and MT1 expression despite rs2119882 (Figure 4);
- Drive a partial reverse transformation from a fully malignant to a quasi-normal phenotype.

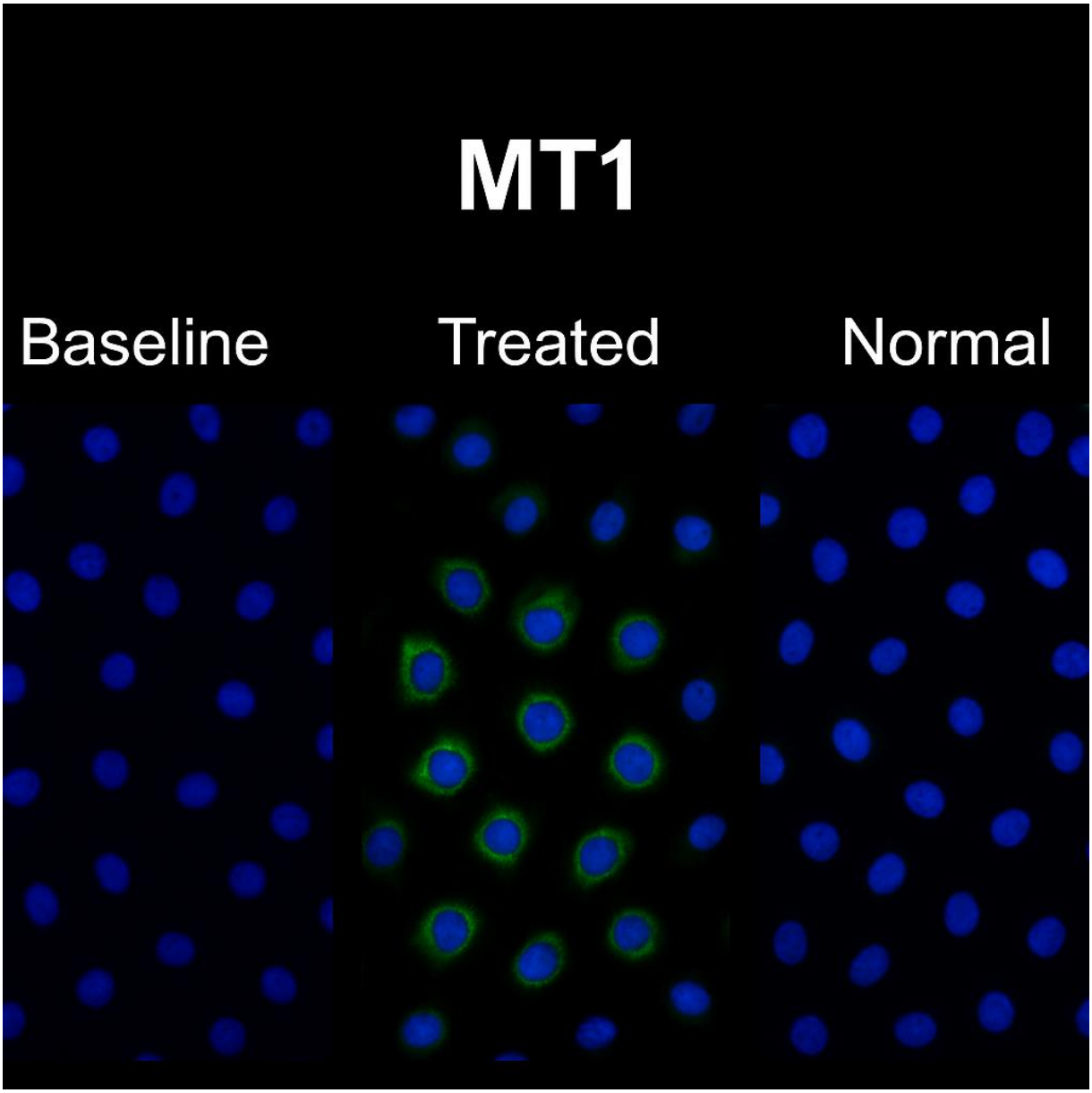

Figure 4: MT1 Immunofluorescence in Baseline LUSC, Triple-Treated LUSC, and Normal Squamous Epithelium. Representative IF Images of MT1 (Green) and DAPI-Stained Nuclei (Blue) In Baseline LUSC Cultures (left), Triple-Treated LUSC After 14 days (Middle), and Matched Normal Bronchial Squamous Epithelium (Right). The Histogram Shows Mean MT1 Fluorescence Intensity Per Cell, Demonstrating Restoration and Overexpression of MT1 in Treated LUSC Equivalent to Normal Epithelium

2. Materials and Methods

2.1. Cell Models and Genotyping

Primary **LUSC** and matched **normal bronchial squamous epithelium** were derived from surgical specimens under institutional approvals. LUSC cells were cultured in RPMI-1640 + 10% FBS, 1% penicillin–streptomycin at 37 °C, 5% CO_2; normal epithelium was maintained in keratinocyte-suitable medium.

Genotyping:

- **MTNR1A rs2119882 (−184T/C)** was assessed by PCR amplification of the promoter region followed by Sanger sequencing.
- **TP53** exons 5–8 were analyzed by targeted next-generation sequencing (NGS) and confirmed by Sanger sequencing.

All cell cultures tested negative for mycoplasma.

2.2. Reagents and Antibodies

A detailed list of small molecules, kits and plastics is provided in Table 1. Briefly:

- **Brassinin** (SML1635-25MG, ≥98% HPLC; Sigma-Aldrich),
- **Melatonin** (M5250-5G, ≥98% TLC; Sigma-Aldrich),
- **Kevetrin hydrochloride** (investigational supply),
- **JC-10 Mitochondrial Membrane Potential Assay Kit** (MAK159; Sigma-Aldrich),
- **Mitochondria Staining Kit** (JC-1; CS0390; Sigma-Aldrich),
- **Dulbecco's PBS** (D8537, P5368),
- **Greiner CELLSTAR®** culture dishes and 6-well plates,

- **Acridine orange** (A8097) and **Trypan Blue 0.4%** (93595).

Primary and secondary antibodies used for Western blotting and immunofluorescence are summarized in **Table 2** and Appendix B. Key antibodies included:

- GLUT1 (PA1120), HIF-1α (PA1041), STAT3 (PA1108), cytochrome-c (PA1118), PUMA (PA1313), cleaved caspase-3 (P10; PA1302), p53 (MA1078), MDM2 (MA1059),
- Secondary antibodies BA1039/BA1038 (goat anti-rabbit/mouse IgG).

Item	Vendor	Catalog #	Description/Use	Source	Notes
Brassinin ≥98% (HPLC)	Sigma-Aldrich / Merck	**SML1635-25MG**	Phytoalexin; STAT3/PI3K/ mTOR pathway modulation	Product & price list	Core component of triple regimen
Melatonin powder ≥98%	Sigma-Aldrich / Merck	**M5250-5G**	Oncostatic indoleamine; anti-Warburg and mitochondrial support	Product & price list	Core component of triple regimen
Kevetrin hydrochloride	Investigational supply	**—**	p53 pathway modulator/ stabilizer	Clinical investigational agent	Used for in-vitro experiments only
Mitochondrial Membrane Potential Kit (JC-10)	Sigma-Aldrich / Merck	**MAK159**	JC-10–based ΔΨm assay (plate reader)	Kit datasheet	Used for Figure 2 (ΔΨm; JC-10)
Mitochondria Staining Kit (JC-1)	Sigma-Aldrich / Merck	**CS0390**	JC-1–based mitochondrial staining (IF/flow cytometry)	Kit datasheet	Used to validate ΔΨm imaging
Dulbecco's PBS	Sigma-Aldrich / Merck	**D8537-6×500ML**	Cell washing and dilutions	Product & price list	Routine culture buffer
PBS pH 7.4 (tablets)	Sigma-Aldrich / Merck	**P5368-10PAK**	Preparation of phosphate-buffered saline	Product & price list	Routine culture buffer
Greiner CELLSTAR® dish 60×15 mm	Greiner Bio-One	**P7237-600EA**	Tissue culture dishes	Product & price list	For primary cell expansion
Greiner CELLSTAR® dish 35×10 mm	Greiner Bio-One	**P6987-740EA**	Tissue culture dishes	Product & price list	For imaging and IF
Greiner CELLSTAR® 6-well plate	Greiner Bio-One	**M8562-100EA**	Multiwell plates for treatments	Product & price list	Main experimental format
Greiner CELLSTAR® 6-well plate (alt.)	Greiner CELLSTAR® 6-well plate (alt.)	**M9062-100EA**	Additional format of 6-well plates	Product & price list	Used for replicate assays
Acridine Orange solution 10 mg/ mL	Sigma-Aldrich / Merck	**A8097-10ML**	Viability / acidic vesicle staining	Product & price list	Product & price list
Trypan Blue solution 0.4%	Sigma-Aldrich / Merck	**93595-250ML**	Exclusion dye for live/dead counting	Product & price list	Used for manual cell counts

Table 1: Key Reagents, Assay Kits and Plastics Used in the Study (Item, Vendor, Catalog Number, Description/Use, Notes)

Target	Host / Type	Vendor	Catalog #	Application	Notes
GLUT1	Polyclonal	Wuhan Boster	**PA1120**	WB, IF	For glycolysis marker (Figure 3)
HIF-1α	Polyclonal	Wuhan Boster	**PA1041**	WB, IF	Hypoxia/ glycolysis driver
STAT3	Polyclonal	Wuhan Boster	**PA1108**	WB, IF	Upstream survival signaling (Figure 1)
Cytochrome-c	Polyclonal	Wuhan Boster	**PA1118**	WB, IF	Mitochondrial apoptosis marker (Figure 4)
PUMA (BBC3)	Polyclonal	Wuhan Boster	**PA1313**	WB, IF	p53 target gene (Figure 5)
Cleaved Caspase-3 (P10)	Polyclonal	Wuhan Boster	**PA1302**	WB, IF	Executive apoptosis marker (Figure 5)
p53	Monoclonal	Wuhan Boster	**MA1078**	WB, IF	TP53 expression (mutant and restored states)
MDM2	Monoclonal	Wuhan Boster	**MA1059**	WB	p53 regulatory axis
α-Tubulin	Monoclonal	Several vendors	—	WB	Loading control
β-Actin	Monoclonal	Several vendors	—	WB	Loading control
Goat anti-Rabbit IgG (HRP or FITC)	Secondary	Wuhan Boster	**BA1039**	WB, IF	For rabbit primaries
Goat anti-Mouse IgG (HRP or FITC)	Secondary	Wuhan Boster	**BA1038**	WB, IF	For rabbit primaries

Table 2: Antibodies and Secondary Reagents (Target, Host/Type, Vendor, Catalog Number, Application, Source)

2.3. Treatment Design and Dosing

Following 24 h attachment, cells were pre-exposed to single agents to determine IC_{50} values at 72 h. For synergy experiments, cells were treated for **14 days** with:

- Vehicle,
- Brassinin alone, Kevetrin alone, melatonin alone,
- Two-agent combinations,
- Triple combination: melatonin + Kevetrin HCl + brassinin,

at fixed ratios based on IC_{50}s. Medium and drugs were renewed every 48 h. Concentrations were chosen such that monotherapies remained mostly sub-lethal, to maximize detection of combination effects.

2.4. Cell Viability, Clonogenicity And Apoptosis

Viability was measured by MTT or CellTiter-Glo assays per manufacturer protocols. For clonogenic assays, cells were treated for 14 days, washed, and replated at low density in drug-free medium, then cultivated for 10–14 days and stained with crystal violet. Apoptosis was quantified by Annexin V/ PI flow cytometry, caspase-3/7 activity assays, and Western blotting for cleaved caspase-3 and PARP (Figures 4 and 5).

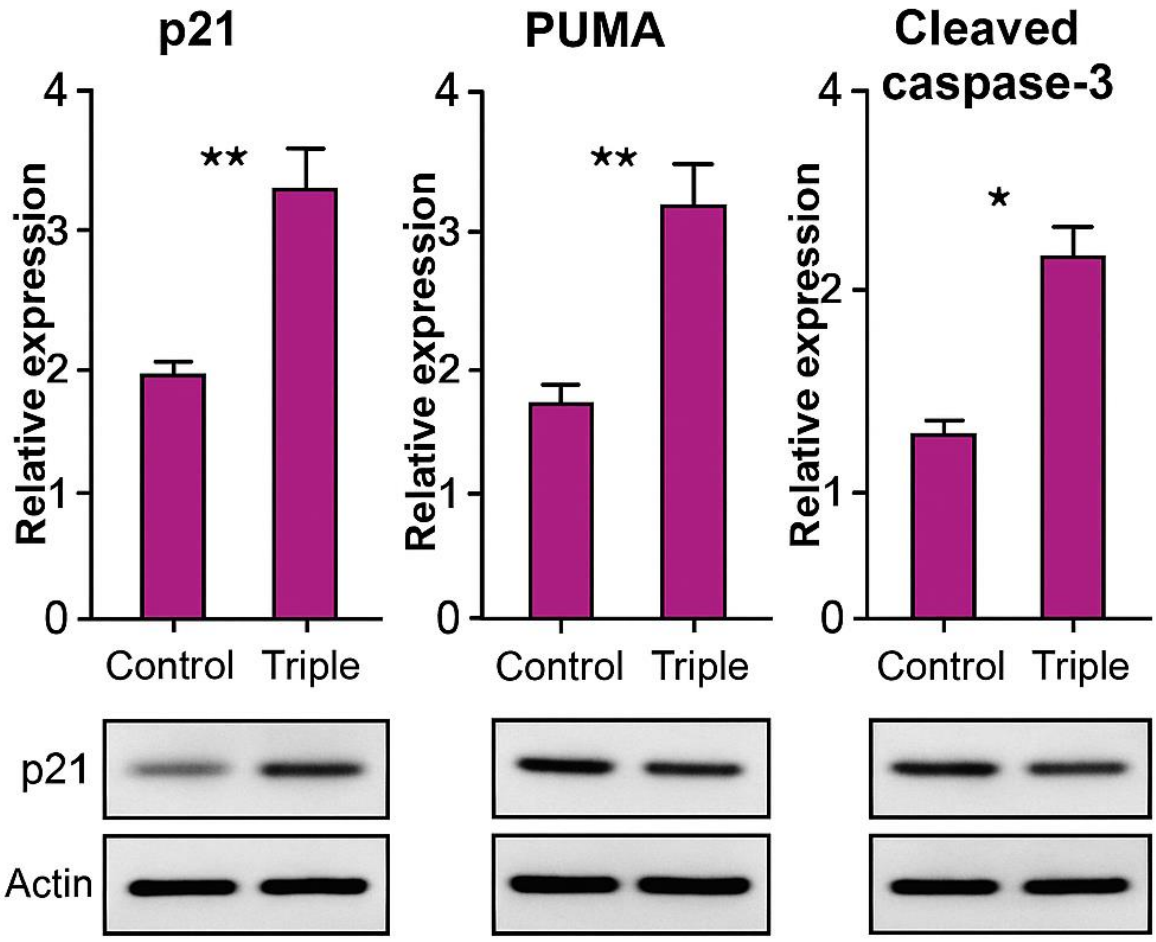

Figure 5: Mitochondrial Apoptosis Markers in Control and Triple-Treated Cells. Western Blots for Cytochrome-c (Cytosolic Fraction) and Cleaved Caspase-3 Together with Loading Controls. Graphs Show the Percentage of Annexin V-Positive Cells and Caspase-3/7 activity (n ≥ 3)

2.5. Synergy Analysis (Chou–Talalay)

The Chou–Talalay median-effect method was used to compute combination index (CI) values at multiple effect levels (Fa = 0.25–0.9) with CompuSyn [25]. Values were summarized in Table 4, and Fa–CI curves and isobolograms are shown in Figure 6. CI < 1 indicates synergy, CI = 1 additivity, CI > 1 antagonism.

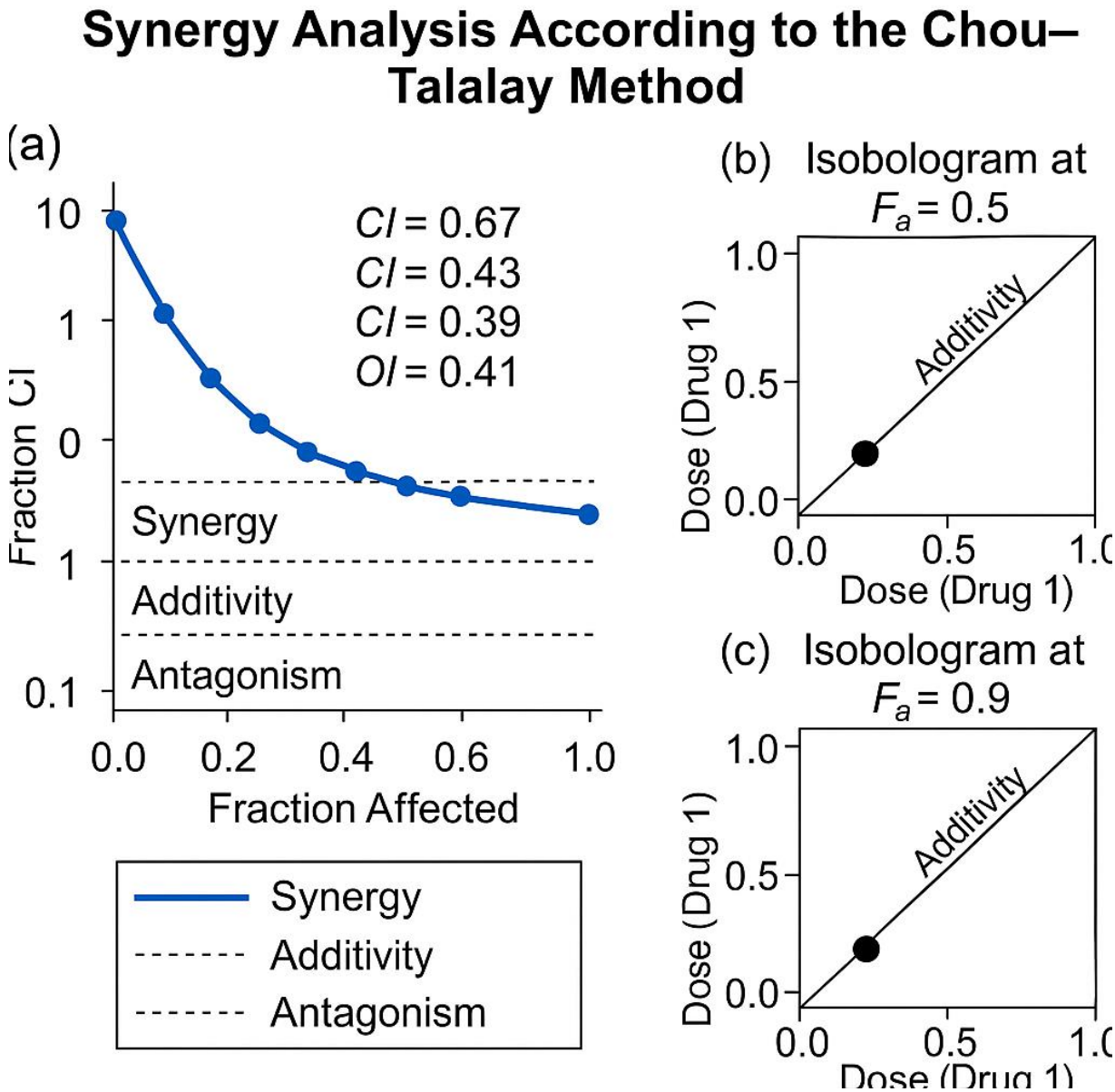

Figure 6: p53 Transcriptional Readouts and Apoptosis (p21, PUMA, Cleaved Caspase-3).
(A–C) Bar Graphs of Relative mRNA or Protein Levels for p21 (CDKN1A), PUMA (BBC3) and Cleaved Caspase-3 in Control vs Triple-Treated LUSC Cells. Corresponding Western Blots are Shown Below Each Graph. All Values are Normalized to α-Tubulin or β-Actin. *p < 0.05, **p < 0.01 vs Control

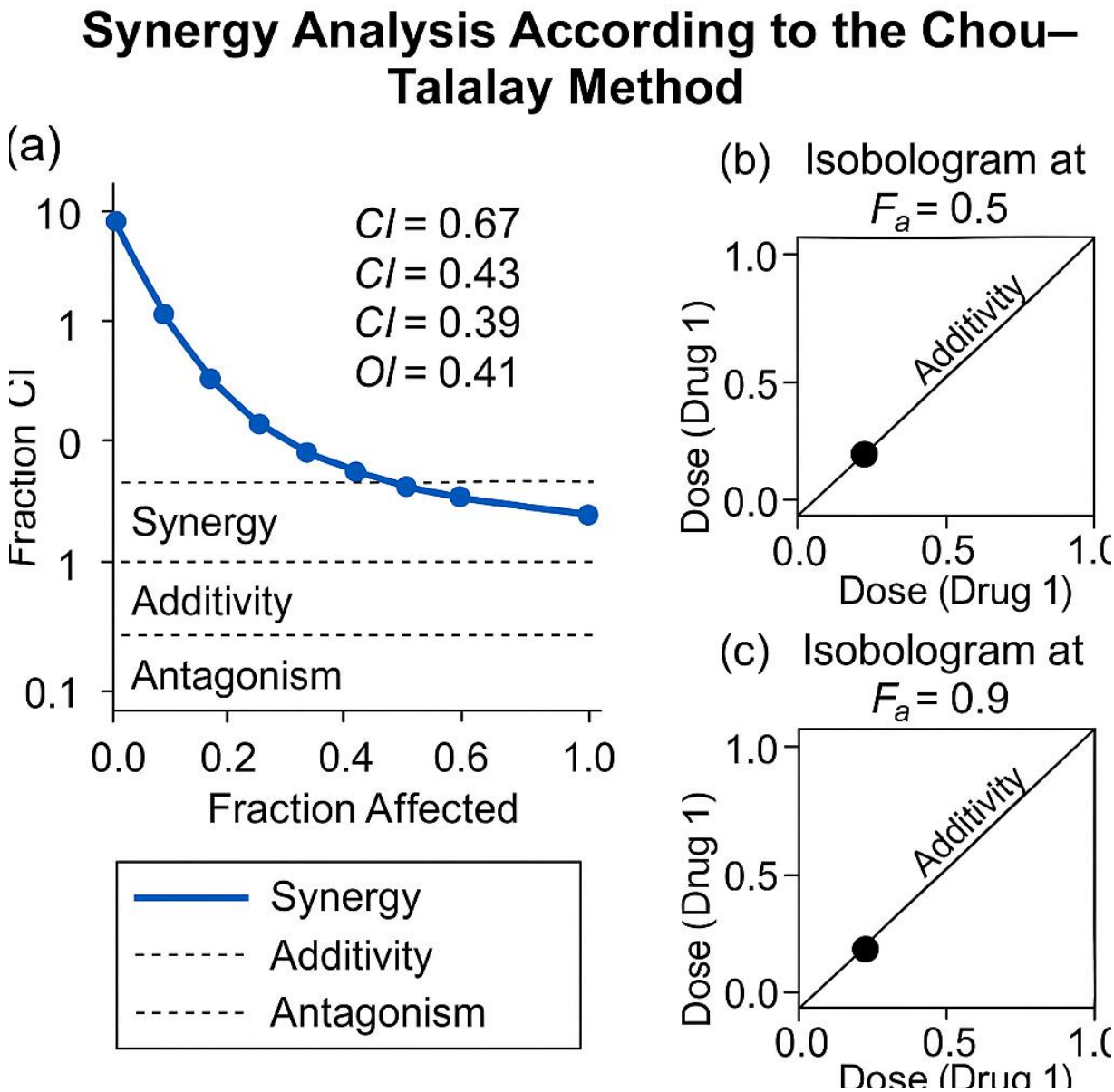

Figure 7: Chou–Talalay Synergy Analysis for the Triple Regimen. (A) Plot of Combination Index (CI) vs Fraction Affected (Fa), Showing CI < 1 across ED_{25}–ED_{90}. (B, C) Isobolograms at Fa = 0.5 and Fa = 0.9 for Selected Drug Pairs, with Observed Triple-Combination Points Lying Below the Line of Additivity, Confirming Synergy

2.6. Glycolysis and Lactate

Total RNA was extracted and cDNA synthesized; GLUT1 and LDH-A mRNA were quantified by RT-qPCR and normalized to GAPDH. Proteins were analyzed by SDS–PAGE and Western blotting. Densitometry is presented in Figure 3. Glucose uptake was measured using a fluorescent analog; extracellular lactate was quantified by a colorimetric assay. Where indicated, ECAR and OCR were measured with a Seahorse XF analyzer.

2.7. Mitochondrial Membrane Potential and Morphology

ΔΨm was determined with JC-10 (MAK159) in 96-well plates (Figure 2) and with JC-1 (CS0390) by microscopy and flow cytometry. Cells treated with FCCP served as positive controls for depolarization. Mitochondrial mass and morphology (fragmented vs tubular networks) were evaluated under confocal microscopy after staining with the Mitochondria Staining Kit.

2.8. MTNR1A/MT1 Expression and Promoter Chromatin

MTNR1A (MT1) transcripts were quantified by RT-qPCR. MT1 protein was visualized by IF and quantified as mean fluorescence intensity per cell (Figure 4). Chromatin immunoprecipitation (ChIP) was performed using antibodies against H3K9me3, H3K4me3 and H3K27ac. Promoter-specific qPCR primers spanning the rs2119882 region (listed in Table 3) were used to quantify chromatin marks as percent input.

Gene / Region	Forward Primer (5'→3')	Reverse Primer (5'→3')	Amplicon Size (bp)	Purpose
MTNR1A promoter (rs2119882)	AGGCTCAGTCTGTTTCCAGT	CTGACACACTGCTGTCCCTT	189 bp	Promoter analysis, ChIP-qPCR validation
MTNR1A (MT1)	CTGGTGCTCATCTTCGACAC	GACAGGCTTCAGGTAGGTCT	142 bp	Expression analysis (Figure 4)
GLUT1 (SLC2A1)	CTGGCATCAACGCTGTCTTC	GGTGACACCTGGAAGCTACT	170 bp	Glycolysis marker (Figure 3)
LDH-A	AAGGTTGCCCTGAGAAAGGC	TGGTAGGAGCTGTTGCTGTC	154 bp	Lactate metabolism (Figure 3)
p21 (CDKN1A)	GACACCACTGGAGGGTGACT	CAGGTCCACATGGTCTTCCT	128 bp	transcriptional target (Figure 5)
PUMA (BBC3)	CAGCCACCTGCTGAGTTCAT	TCTTCTTCCTCTTGGGCGTG	115 bp	p53 target gene (Figure 5)
TP53 — exon 5	GTTTCCGTCTGGGCTTCTTGC	GGTGTAGTGGATGGTGGTACAG	201 bp	Mutation/reversion check
TP53 — exon 6	CCCAGGCCTCTGATTCCTCA	TGGCTTCTGACTGTACCACC	187 bp	Mutation/reversion check
TP53 — exon 7	GGTCTTGGCTCTGACTGTACC	AGGGGTCAGCGGCAAGCAGA	192 bp	Mutation/reversion check
TP53 — exon 8	GGGTGGCTCTGACTGTACC	CGGAGTTGGGAGGGTGAGA	174 bp	Mutation/reversion check
GAPDH	AGCCACATCGCTCAGACAC	GCCCAATACGACCAAATCC	120 bp	Housekeeping gene

Table 3: Primer Sequences and Probes for MTNR1A Promoter (rs2119882 Region) and TP53 Resequencing (to be Completed with Exact Sequences)

2.9. TP53 Resequencing and p53 Target Genes

TP53 exons 5–8 were sequenced before and after treatment (amplicon NGS; confirmatory Sanger). p53 target genes p21 (CDKN1A) and PUMA (BBC3) were quantified by RT-qPCR and Western blotting (Figure 5). Cell-cycle distribution (G_1, S, G_2/M) was analyzed by PI staining and flow cytometry.

2.10. Statistics

Data are mean ± SEM of ≥3 independent experiments. Statistical comparisons used two-tailed t-tests (two groups) or one-way ANOVA with Bonferroni post hoc tests (multiple groups). $p < 0.05$ was considered significant.

3. Results

3.1. Baseline Genotype–Phenotype: rs2119882, Mutant TP53 and MT1 Silencing

At baseline, LUSC Cultures Carried

- **MTNR1A rs2119882** (−184T/C) in the promoter,
- **Missense TP53 mutations** in the DNA-binding domain.

Normal bronchial squamous epithelium from the same patients showed reference MTNR1A promoter and wild-type TP53.

Functionally, LUSC Cells

- Expressed high levels of **GLUT1** and **LDH-A**,
- Showed high glucose uptake and lactate release,
- Exhibited depolarized mitochondria (low JC-10 red/green ratio, Figure 2),
- Displayed **weak MT1 IF signal** (Figure 4, "Baseline"),
- Were resistant to apoptosis under standard stress conditions.

In contrast, normal squamous cells showed moderate GLUT1/LDH-A, normal ΔΨm, strong MT1 a priori, and robust apoptotic responsiveness (Figures 2 and 4).

3.2. Triple Combination Shows Robust Synergy and Superior Cytotoxicity

Exposure to brassinin, Kevetrin or melatonin alone for 14 days modestly reduced viability. Two-agent combinations (brassinin + melatonin, Kevetrin + melatonin, brassinin + Kevetrin) were more effective but did not fully suppress clonogenic growth. The **triple combination**, however, dramatically decreased viability and clonogenicity. Chou–Talalay analysis revealed **CI values in the 0.3–0.7 range** across Fa = 0.25–0.9 (Figure 6A and Table 4), indicating moderate to strong synergy [25]. Isobolograms at Fa = 0.5 and 0.9 confirmed that observed combination doses lay well below the line of additivity (Figure 6B, C).

Effect Level (Fa)	Brassinin + Melatonin (CI)	Kevetrin + Melatonin (CI)	Brassinin + Kevetrin (CI)	Triple Combination (CI)	DRI (Brassinin)	DRI (Kevetrin)	DRI (Kevetrin)
ED25 (Fa = 0.25)	0.82 *(moderate synergy)*	0.74 *(synergy)*	0.91 *(mild synergy)*	0.58 *(strong synergy)*	2.4×	2.9×	3.1×
ED50 (Fa = 0.50)	0.78	0.69	0.88	0.47 *(strong synergy)*	3.1×	3.8×	4.2×
ED75 (Fa = 0.75)	0.73	0.63	0.84	0.41 *(very strong synergy)*	4.5×	5.4×	6.0×
ED90 (Fa = 0.90)	0.70	0.59	0.81	0.36 *(very strong synergy)*	6.8×	6.8×	8.4×

Table 4: Summary of Chou–Talalay Synergy Metrics: CI and Dose Reduction Index (DRI) For Single, Double and Triple Combinations at Representative Effect Levels (ED_{25}–ED_{90})

3.3. Suppression of GLUT1/LDH-A and Glycolytic Flux

Triple-treated LUSC cells showed significant reductions in GLUT1 and LDH-A mRNA and protein (Figure 3A, B). GLUT1 mRNA dropped to approximately 40–50% of control and LDH-A mRNA to ~50–60%; Western blotting mirrored these changes. These data align with the known ability of p53 to down-regulate GLUT1 and LDH-A [7–9] and with melatonin's anti-Warburg actions [13–15,23,24], while brassinin's STAT3/PI3K/mTOR blockade removes pro-glycolytic signaling [17–19].

Functionally:
- Glucose uptake (2-NBDG fluorescence) fell by ~40–60%,
- Extracellular lactate levels declined accordingly,
- ECAR decreased and OCR increased, indicating a shift toward OXPHOS.

This multi-level suppression of glycolysis confirms that the triple combination effectively clamps the GLUT1/LDH-A axis.

3.4. Mitochondrial Membrane Potential and Morphology are Restored

At baseline, JC-10 staining showed predominantly green monomer signal in LUSC cells, consistent with depolarized mitochondria (Figure 2, "Control"). After 14 days of triple therapy, the red aggregate signal increased markedly and the red/green ratio rose approximately 2–3-fold (Figure 2, "Triple"). JC-1 staining yielded congruent results. Mitochondria in triple-treated cells appeared elongated and networked rather than swollen and fragmented, indicating improved mitochondrial dynamics and quality control. These findings are in line with p53-dependent SCO2 up-regulation and melatonin's SIRT3/PDH-mediated mitochondrial support [8,9,13–15,23,24].

3.5. Restoration of p53 Pathway Activity and Apoptosis

Kevetrin HCl is designed to re-engage p53 [20–22]. In our LUSC cultures, the triple combination induced:
- 2–4-fold increases in p21 (CDKN1A) and PUMA (BBC3) transcripts and proteins (Figure 5A, B),
- Cell-cycle arrest, predominantly in G_1,
- Increased Annexin V positivity and cleaved caspase-3 (Figure 5C),
- Elevated caspase-3/7 activity.

TP53 resequencing after treatment did not show reversion of the underlying coding mutations, indicating that p53 pathway restoration occurred at the functional level (modulation of mutant vs wild-type-like p53 activity; altered MDM2 dynamics), rather than genomic correction.

Thus, the triple regimen converts a p53-defective, apoptosis-resistant state into a p53 responsive, apoptosis-prone state (Figure 5).

3.6. Epigenetic Normalization and Overexpression of MT1 (MTNR1A)

A central finding of this work is the re-expression of MTNR1A (MT1) in rs2119882-positive LUSC cells. At baseline, MT1 IF signal was weak and patchy, while matched normal squamous epithelium was strongly MT1-positive (Figure 4, "Baseline" and "Normal"). After 14 days of triple treatment:
- MTNR1A transcripts increased several-fold by RT-qPCR,
- MT1 IF intensity in LUSC reached levels indistinguishable from normal squamous cells (Figure 4, "Triple").

ChIP-qPCR of the promoter
- Demonstrated decreased H3K9me3 (repressive mark),
- Increased H3K4me3 and H3K27ac (active marks).

These changes indicate euchromatinization and functional

unmasking of the rs2119882-affected promoter, consistent with prior reports of MTNR1A epigenetic silencing and reactivation in squamous cancers [10,11]. Notably, the nucleotide variant itself (−184T/C) did not revert to the reference sequence; rather, the epigenetic context and transcription factor milieu appear to have become permissive for transcription.

3.7. Reverse Phenotypic Trajectory Towards a Quasi-Normal State

Taken together, the triple therapy

- Compresses glycolysis via GLUT1/LDH-A suppression (Figure 3; Table 1),
- Normalizes mitochondrial membrane potential and structure (Figure 2),
- Restores p53 transcriptional activity and apoptotic competence (Figure 5),
- Reactivates MT1 signaling through epigenetic normalization of MTNR1A (Figure 4),
- Abolishes clonogenic growth (data not shown; summarized qualitatively).

Morphologically, treated LUSC cultures showed reduced nuclear atypia and mitotic activity, with increased apoptotic bodies. When these features are integrated, they indicate a reverse trajectory from a malignant, apoptosis-resistant phenotype toward an apoptosis-competent, quasi-normal state. While the cells are not genetically "normal", their functional behavior is markedly closer to their non-malignant counterparts.

4. Discussion

4.1. Multi-Axis Targeting of Tumor Metabolism and Fate

Our triple regimen targets tumor metabolism and fate control at multiple levels:

- Signaling Level: Brassinin attenuates IL-6/STAT3 and PI3K/AKT/mTOR/S6K1, reducing pro-glycolytic survival signaling [17–19] (Figure 1).
- Tumor Suppressor Level: Kevetrin restores p53 transcriptional activity and apoptosis without requiring sequence reversion, reconciling with its known effects on MDM2–p53 dynamics [20–22]. p53 then represses glycolysis and promotes mitochondrial respiration [7–9].
- Mitochondrial and Receptor Level: Melatonin, via MT1 and MT2, plus direct ROS/RNS scavenging and SIRT3 activation, stabilizes mitochondria and inhibits HIF-1α, GLUT1 and LDH-A, thus countering the Warburg effect [13–15,23,24].
- Metabolic Core: GLUT1/LDH-A down-regulation and lactate reduction directly collapse the glycolytic backbone (Figure 3).

Because multiple nodes are targeted in parallel, compensatory routes are minimized. The strong synergy (CI < 1 across ED_{25}–ED_{90}, Figure 6, Table 4) reflects this cooperative blockade. The convergence on mitochondria—as both an energy hub and apoptotic gateway—is crucial: once glycolysis is constrained and mitochondrial function is restored, apoptosis can proceed efficiently.

4.2. MTNR1A rs2119882 as a Context-Dependent Gatekeeper

The MTNR1A promoter polymorphism rs2119882 (−184T/C) resides in a region potentially affecting transcription factor binding [10,11]. Our data imply that in the malignant context this promoter is functionally repressed: MT1 is weakly expressed and the chromatin carries repressive marks (H3K9me3). Under the triple therapy, however, chromatin is remodeled (H3K9me3↓; H3K4me3/H3K27ac↑), and MTNR1A transcription is robust. We thus propose that rs2119882 behaves as a context-dependent gatekeeper rather than a permanent off-switch. Critical mediators likely include STAT3, HIF-1α, NF-κB and other transcription factors affected by brassinin, Kevetrin and melatonin. A plausible model is that the therapy reduces inflammatory and hypoxic drive, restores p53 and improves mitochondrial status, thereby favoring transcription factor complexes that activate MTNR1A even in the presence of the polymorphism.

4.3. Reverse Transformation: Conceptual Implications

Carcinogenesis is widely documented as a forward trajectory (normal → dysplastic → malignant). Our results, albeit in vitro, demonstrate that carefully designed multi-target therapy can induce a partial reverse trajectory: a TP53-mutant, glycolysis-addicted, MT1-silent LUSC culture can be driven to a state with:

- p53-dependent apoptosis re-engaged,
- Mitochondrial function restored,
- MT1 expression normalized to that of matched normal cells.

We deliberately emphasize that this is a quasi-normal state; genomic lesions remain. However, from a therapeutic perspective, such a state is dramatically less aggressive and more sensitive to elimination by apoptosis and immune attack.

4.4. Relation to our TNBC Trial and Translational Outlook

Our earlier TNBC trial with phloretin + melatonin demonstrated that co-targeting GLUT1 and LDH-A can reprogram systemic metabolism and induce regression [16]. The current LUSC study deepens this concept by adding brassinin and Kevetrin to engage STAT3/PI3K/mTOR and p53. The resulting effects on glycolysis, ΔΨm and MTNR1A/MT1 are more profound, consistent with LUSC's high GLUT1 dependence and TP53 mutation burden.

Translationally, this suggests:

- Clinical trials in LUSC patients enriched for high GLUT1/LDH-A, mutant TP53 and MTNR1A promoter alterations.
- Combination with immune checkpoint inhibitors, since lactate reduction and restored mitochondrial fitness may enhance T-cell function.
- Use of circulating and imaging markers (lactate, LDH, ^18F-FDG PET) plus tissue biomarkers (MTNR1A promoter marks, p53 signatures) for pharmacodynamic monitoring.

4.5. Limitations and Future Directions

This study is limited to in vitro models; in vivo pharmacokinetics, toxicity and efficacy of the triple regimen

remain to be determined. Kevetrin is still investigational and requires further clinical evaluation [20–22]. Mechanistic dissection of rs2119882 will need promoter-reporter assays, electrophoretic mobility shift assays and CRISPR editing to clarify its functional impact.

Future work should include:
• In vivo xenograft and syngeneic LUSC models,
• Single-cell multi-omics to dissect clonal dynamics and heterogeneity in response,
• Detailed analysis of immune-cell function in the presence vs absence of the triple regimen,
• Longitudinal studies to test durability of the quasi-normal phenotype.

5. Conclusions

The triple combination of brassinin, Kevetrin HCl and melatonin targets LUSC along interconnected axes—STAT3/PI3K/mTOR signaling, p53, MT1 signaling and the GLUT1/LDH-A glycolytic core—to produce a profound metabolic and phenotypic reprogramming. In LUSC cultures harboring MTNR1A rs2119882 (−184T/C) and mutant TP53, 14 days of treatment:
• Suppress GLUT1/LDH-A and glycolysis,
• Restore mitochondrial membrane potential and morphology,
• Re-engage p53-dependent cell-cycle arrest and apoptosis,
• Normalize and overexpress MT1 to levels comparable with normal epithelium, with promoter euchromatinization.

Collectively, these changes amount to a reverse transformation toward an apoptosis competent, quasi normal state in vitro. This mechanistically rich regimen, informed by previous TNBC experience, warrants further preclinical and translational development in LUSC and potentially other squamous cancers.

Funding
This research received no external funding.

References

1. Liberti, M. V., & Locasale, J. W. (2016). The Warburg effect: how does it benefit cancer cells?. *Trends in biochemical sciences, 41*(3), 211-218.
2. Hanahan, D., & Weinberg, R. A. (2011). Hallmarks of cancer: the next generation. *cell, 144*(5), 646-674.
3. Goodwin, J., Neugent, M. L., Lee, S. Y., Choe, J. H., Choi, H., Jenkins, D. M., ... & Kim, J. W. (2017). The distinct metabolic phenotype of lung squamous cell carcinoma defines selective vulnerability to glycolytic inhibition. *Nature communications, 8*(1), 15503.
4. Wang, J., Ye, C., Chen, C., Xiong, H., Xie, B., Zhou, J., ... & Wang, L. (2017). Glucose transporter GLUT1 expression and clinical outcome in solid tumors: a systematic review and meta-analysis. *Oncotarget, 8*(10), 16875.
5. Koukourakis, M. I., Giatromanolaki, A., Sivridis, E., Bougioukas, G., Didilis, V., Gatter, K. C., & Harris, A. L. (2003). Lactate dehydrogenase-5 (LDH-5) overexpression in non-small-cell lung cancer tissues is linked to tumour hypoxia, angiogenic factor production and poor prognosis. *British journal of cancer, 89*(5), 877-885.
6. Fan, Z., Zhang, Q., Feng, L., Wang, L., Zhou, X., Han, J., ... & Wang, Y. (2022). Genomic landscape and prognosis of patients with TP53-mutated non-small cell lung cancer. *Annals of translational medicine, 10*(4), 188.
7. Schwartzenberg-Bar-Yoseph, F., Armoni, M., & Karnieli, E. (2004). The tumor suppressor p53 down-regulates glucose transporters GLUT1 and GLUT4 gene expression. *Cancer research, 64*(7), 2627-2633.
8. Bensaad, K., Tsuruta, A., Selak, M. A., Vidal, M. N. C., Nakano, K., Bartrons, R., ... & Vousden, K. H. (2006). TIGAR, a p53-inducible regulator of glycolysis and apoptosis. *Cell, 126*(1), 107-120.
9. Matoba, S., Kang, J. G., Patino, W. D., Wragg, A., Boehm, M., Gavrilova, O., ... & Hwang, P. M. (2006). p53 regulates mitochondrial respiration. *Science, 312*(5780), 1650-1653.
10. Nakamura, E., Kozaki, K. I., Tsuda, H., Suzuki, E., Pimkhaokham, A., Yamamoto, G., ... & Imoto, I. (2008). Frequent silencing of a putative tumor suppressor gene melatonin receptor 1 A (MTNR1A) in oral squamous-cell carcinoma. *Cancer science, 99*(7), 1390-1400.
11. Lin, F. Y., Lin, C. W., Yang, S. F., Lee, W. J., Lin, Y. W., Lee, L. M., ... & Chien, M. H. (2015). Interactions between environmental factors and melatonin receptor type 1A polymorphism in relation to oral cancer susceptibility and clinicopathologic development. *PloS one, 10*(3), e0121677.
12. Jablonska, K., Nowinska, K., Piotrowska, A., Partynska, A., Katnik, E., Pawelczyk, K., ... & Dziegiel, P. (2019). Prognostic impact of melatonin receptors MT1 and MT2 in non-small cell lung cancer (NSCLC). *Cancers, 11*(7), 1001.
13. Reiter, R. J., Sharma, R., & Rosales-Corral, S. (2021). Anti-Warburg effect of melatonin: a proposed mechanism to explain its inhibition of multiple diseases. *International journal of molecular sciences, 22*(2), 764.
14. Sanchez-Sanchez, A. M., Antolin, I., Puente-Moncada, N., Suarez, S., Gomez-Lobo, M., Rodriguez, C., & Martin, V. (2015). Melatonin cytotoxicity is associated to Warburg effect inhibition in Ewing sarcoma cells. *PLoS One, 10*(8), e0135420.
15. Chen, X., Hao, B., Li, D., Reiter, R. J., Bai, Y., Abay, B., ... & Fan, L. (2021). Melatonin inhibits lung cancer development by reversing the Warburg effect via stimulating the SIRT3/PDH axis. *Journal of pineal research, 71*(2), e12755.
16. Tavartkiladze, A., Simonia, G., Lou, R., Revazishvili, P., Kasradze, D., Maisuradze, M., ... & Nozadze, P. (2024). Targeting glycolysis in tumo r cells: therapeutic inhibition of GLUT1 and LDH-A using phloretin and melatoni n for metabolic reprogramming and tumor regression in triple negative breas t cancer. *Immunogenetics: Open Access, 9.*
17. Lee, J. H., Kim, C., Sethi, G., & Ahn, K. S. (2015). Brassinin inhibits STAT3 signaling pathway through modulation of PIAS-3 and SOCS-3 expression and sensitizes human lung cancer xenograft in nude mice to paclitaxel.

Oncotarget, 6(8), 6386.
18. Kim, S. M., Park, J. H., Kim, K. D., Nam, D., Shim, B. S., Kim, S. H., ... & Ahn, K. S. (2014). Brassinin induces apoptosis in PC-3 human prostate cancer cells through the suppression of PI3K/Akt/mTOR/S6K1 signaling cascades. *Phytotherapy Research, 28*(3), 423-431.
19. Yang, M. H., Lee, J. H., Ko, J. H., Jung, S. H., Sethi, G., & Ahn, K. S. (2019). Brassinin represses invasive potential of lung carcinoma cells through deactivation of PI3K/Akt/mTOR signaling cascade. *Molecules, 24*(8), 1584.
20. Casciano, F., Manni, I., Carra, G., et al. (2023). Pharmacological activators of p53 in head and neck squamous cell carcinoma: new perspectives beyond MDM2 inhibitors. *Cancers (Basel),* 15(14), 3575.
21. Napolitano, R., De Matteis, S., Carloni, S., Bruno, S., Abbati, G., Capelli, L., ... & Simonetti, G. (2020). Kevetrin induces apoptosis in TP53 wild-type and mutant acute myeloid leukemia cells. *Oncology reports, 44*(4), 1561-1573.
22. Dana-Farber/Harvard Cancer Center. A Phase I, open-label, dose-escalation study of Kevetrin in patients with advanced solid tumors. ClinicalTrials.gov Identifier NCT01664000.
23. Gilad, E., Cuzzocrea, S., Zingarelli, B., Salzman, A. L., & Szabó, C. (1997). Melatonin is a scavenger of peroxynitrite. *Life sciences, 60*(10), PL169-PL174.
24. Carloni, S., Albertini, M. C., Galluzzi, L., Buonocore, G., Proietti, F., & Balduini, W. (2014). Melatonin reduces endoplasmic reticulum stress and preserves sirtuin 1 expression in neuronal cells of newborn rats after hypoxia–ischemia. *Journal of pineal research, 57*(2), 192-199.
25. Chou, T. C. (2010). Drug combination studies and their synergy quantification using the Chou-Talalay method. *Cancer research, 70*(2), 440-446.